

# Ab Initio Characterization of the Structure, Vibrational, and Energetic Properties of $\text{Br}^- \cdot \text{HOCl}$ , $\text{Cl}^- \cdot \text{HOBr}$ , and $\text{Br}^- \cdot \text{HOBr}$ Anionic Complexes

Bradley A. Flowers and Joseph S. Francisco\*

Department of Chemistry and Department of Earth and Atmospheric Sciences, Purdue University, West Lafayette, Indiana 47907-1393

Received: September 14, 2000; In Final Form: November 7, 2000

Ab initio molecular orbital methods have been employed to determine molecular structure, vibrational frequencies, and relative energetics of  $\text{Br}^- \cdot \text{HOCl}$ ,  $\text{Cl}^- \cdot \text{HOBr}$ , and  $\text{Br}^- \cdot \text{HOBr}$  anionic complexes. These parameters were determined using second-order Møller–Plesset perturbation theory (MP2) and coupled cluster methods. The minimum energy structures for all three complexes are reported. The minima for the mixed halogen conformers place the halogen anion in complexation through the hydrogen. The calculated binding energies are 23.3, 19.5, and 19.5 kcal mol<sup>-1</sup> for  $\text{Cl}^- \cdot \text{HOBr}$ ,  $\text{Br}^- \cdot \text{HOCl}$ , and  $\text{Br}^- \cdot \text{HOBr}$ , respectively.

## I. Introduction

Heterogeneous reactions on the surface of polar stratospheric clouds (PSCs) are believed to be a primary means for activation of bromine and chlorine radicals during the polar spring. Hypochlorous acid, HOCl, which is present in trace amounts in the stratosphere, is produced by the hydrolysis of chlorine nitrate ( $\text{ClONO}_2$ ) on the surface of PSCs during the polar winter by the following reaction:<sup>1–3</sup>



Reaction 1 produces HOCl very rapidly, thus contributing to the springtime development of the Antarctic ozone “hole”. Hypobromous acid, HOBr, is also present in trace concentrations in the stratosphere. It is also formed in a similar manner on the surface of PSCs during the dark polar winter.<sup>4,5</sup>



Experimental groups have explained the consequent loss of ozone in the polar spring to a continued reaction of the HOCl and HOBr formed in reactions 1 and 2, with HCl and HBr species present in PSCs. The kinetics and reactive uptake of these reactions have been thoroughly examined.<sup>6–11</sup> Important heterogeneous processes that involve HOCl and HOBr are given below. Each reaction converts a stable halogen reservoir species into the photochemically active form of the halogen. These reactions have been found to involve bromine and chlorine in the same reaction, as well as reactions involving only chlorinated and brominated species.



While it is accepted that this type of reactivity takes place on



PSCs, the mechanism of this reaction remains to be determined. The presence of  $\text{Cl}^-$  on PSCs is known to catalyze the

conversion of  $\text{ClONO}_2$  to photochemically active  $\text{Cl}_2$ .<sup>12–14</sup> Theoretical studies have indicated that the presence of  $\text{Cl}^-$  could have a similar impact on the conversion of HOCl to  $\text{Cl}_2$ .<sup>15,16</sup> Eigen and Kustin<sup>17</sup> have proposed a general mechanism for this conversion. Using reaction 3, an example is shown below:



Chu and Chu<sup>11</sup> have suggested an analogous mechanism for



the heterogeneous reaction of  $\text{HOCl} + \text{HBr} \rightarrow \text{BrCl} + \text{H}_2\text{O}$ , shown below.



In an effort to further elucidate this important reactivity, we



report ab initio calculations pertaining to the structure, vibrational frequencies, and relative energetics of complexes similar to those in reactions 7–9. We seek to determine the binding location of the halogen anion to the acid and whether the anion prefers to attach to the hydrogen or the halogen in the acid. Where possible, we have included comparison data from experiments. Also, to serve as another point of comparison, we have included calculations and data from  $\text{Cl}^- \cdot \text{H}_2\text{O}$  and  $\text{Br}^- \cdot \text{H}_2\text{O}$  complexes.

## II. Calculation Method

Ab initio molecular orbital calculations were performed using the GAUSSIAN 94 package of programs.<sup>18</sup> All geometries were fully optimized using second-order Møller–Plesset perturbation theory (MP2)<sup>19</sup> and coupled cluster theory using single and double excitation, along with a perturbational estimation of triplet excitation [CCSD(T)].<sup>20</sup> The optimizations are performed using one basis set of double- $\zeta$  quality, 6-31G(d), and two basis sets of triple- $\zeta$  quality, 6-311G(d,p) and 6-311++G(2df,2p). Vibrational frequencies were computed numerically with a 6-311G(d,p) basis set at the CCSD(T) level of theory.

## III. Results and Discussion

**A. Calibration Calculations  $\text{Cl}^- \cdot \text{H}_2\text{O}$  and  $\text{Br}^- \cdot \text{H}_2\text{O}$ .** To our knowledge, there have been no previous studies on the

**TABLE 1: Geometries<sup>a</sup> at Various Levels of Theory for Cl<sup>-</sup>·H<sub>2</sub>O and Br<sup>-</sup>·H<sub>2</sub>O Anion Cluster**

species	level of theory	geometric parameters				
		r(H'O)	r(OH)	r(H'X)	θ(XHO)	θ(HOH)
Cl <sup>-</sup> ·H <sub>2</sub> O	MP2/6-31G(d)	0.989	0.968	2.227	160.9	99.4
	MP2/6-311G(d,p)	0.976	0.958	2.219	159.7	98.2
	MP2/6-311++G(2df,2p)	0.988	0.957	2.102	168.7	100.9
	CCSD(T)/6-31G(d)	0.988	0.971	2.249	160.4	99.4
	CCSD(T)/6-311G(d,p)	0.975	0.959	2.233	159.9	98.3
	CCSD(T)/6-311++G(2df,2p)	0.985	0.958	2.132	167.7	100.9
Br <sup>-</sup> ·H <sub>2</sub> O	MP2/6-31G(d)	0.986	0.969	2.403	156.5	99.1
	MP2/6-311G(d,p)	0.971	0.958	2.432	154.6	97.9
	MP2/6-311++G(2df,2p)	0.980	0.957	2.324	165.9	100.9
	CCSD(T)/6-31G(d)	0.986	0.971	2.434	155.2	99.0
	CCSD(T)/6-311G(d,p)	0.971	0.959	2.450	154.0	98.0
	CCSD(T)/6-311++G(2df,2p)	0.979	0.959	2.367	164.3	100.8

<sup>a</sup> All bond distances are reported in angstroms and bond angles in degrees.

**TABLE 2: Vibrational Frequencies (cm<sup>-1</sup>) for Cl<sup>-</sup>·H<sub>2</sub>O and Br<sup>-</sup>·H<sub>2</sub>O Anion Cluster<sup>a</sup>**

species	mode no.	mode symmetry	mode description	CCSD(T)/6-311G(d,p)	exp
Cl <sup>-</sup> ·H <sub>2</sub> O	1	a'	HO stretch, uncomplexed	3785	3698 <sup>b</sup>
	2		HO stretch, complexed	3524	3285 <sup>b</sup> , 3103 <sup>c</sup>
	3		HOH bend	1806	
	4		H <sub>2</sub> O in-plane rock	325	
	5		Cl-H' stretch	191	
	6	a''	H bonded to the ion	736	
Br <sup>-</sup> ·H <sub>2</sub> O	1	a'	HO stretch, uncomplexed	3945	
	2		HO stretch, complexed	3565	3368 <sup>d</sup>
	3		HOH bend	1736	
	4		H <sub>2</sub> O in-plane rock	368	
	5		Br-H' stretch	169	
	6	a''	H bonded to the ion	700	

<sup>a</sup> Experimental frequencies for H<sub>2</sub>O: 3943, 3832, 1648 cm<sup>-1</sup>. <sup>b</sup> Reference 18 <sup>c</sup> Reference 21. <sup>d</sup> Ayotte, P.; et al. *J. Phys. Chem.* **1998**, *102*, 3067.

anionic Br<sup>-</sup>·HOCl or Cl<sup>-</sup>·HOBr systems. Thus, to calibrate our calculations, we have performed geometry optimization and harmonic frequency calculations on Cl<sup>-</sup>·H<sub>2</sub>O and Br<sup>-</sup>·H<sub>2</sub>O anionic complexes, for which there are numerous theoretical and experimental studies.

Molecular geometries have been fully optimized at all levels of theory. Our best estimate of the equilibrium geometry for Cl<sup>-</sup>·H<sub>2</sub>O is at the CCSD(T)/6-311++G(2df,2p) level. Our results are in good agreement with previous ab initio efforts. For instance, we report a Cl-H' bond length of 2.132 Å at the CCSD(T)/6-311++G(2df,2p) level. This corresponds well to the 2.151 Å value reported by Choi et al.<sup>18</sup> at the MP2/6-311++G\*\* level. Also, this value is in agreement with the 2.115 Å value determined by Combariza et al.<sup>19</sup> using density functional methods. For the H'O bond, Combariza and Kestner<sup>19</sup> report a value of 0.96 Å. This is in excellent agreement with our result of 0.958 Å at the CCSD(T)/6-311++G(2df,2p) level. Our best estimation of the H'OH angle is 100.9°. Combariza et al.<sup>19</sup> report a similar value of 102.3° from their density functional study, and our value is also in agreement with 100.6° reported by Xantheas<sup>20</sup> with an MP4/aug-cc-pVTZ basis set. The complete results from these calculations are provided in Table 1.

We report harmonic vibrational frequencies for Cl<sup>-</sup>·H<sub>2</sub>O in Table 2. These frequencies were calculated for the C<sub>s</sub> minimum energy conformation. All frequencies are predicted to be positive, real numbers, which indicate that the C<sub>s</sub> structure is truly a minimum energy structure on the Cl<sup>-</sup>·H<sub>2</sub>O potential energy surface. For Cl<sup>-</sup>·H<sub>2</sub>O, we report six normal vibrational modes. The modes ν<sub>1</sub> and ν<sub>2</sub> are the uncomplexed and complexed OH stretches, respectively. The ν<sub>3</sub> mode corresponds to the HOH bending frequency, and ν<sub>4</sub> is the HOH in-plane rocking motion. The fifth and sixth modes (ν<sub>5</sub> and ν<sub>6</sub>) correspond to the chlorine anion bonded to H', and to the out-of-plane

**TABLE 3: Relative Energetics for Cl<sup>-</sup>·H<sub>2</sub>O and Br<sup>-</sup>·H<sub>2</sub>O Anion Cluster<sup>a</sup>**

species	level of theory	X <sup>-</sup> ·H <sub>2</sub> O → X <sup>-</sup> + H <sub>2</sub> O
Cl <sup>-</sup> ·H <sub>2</sub> O	MP2/6-31G(d)	15.4
	MP2/6-311G(d,p)	12.9
	MP2/6-311++G(2df,2p)	14.4
	CCSD(T)/6-31G(d)	15.0
	CCSD(T)/6-311G(d,p)	12.7
	CCSD(T)/6-311++G(2df,2p)	14.1
Br <sup>-</sup> ·H <sub>2</sub> O	MP2/6-31G(d)	15.9
	MP2/6-311G(d,p)	12.3
	MP2/6-311++G(2df,2p)	12.0
	CCSD(T)/6-31G(d)	15.3
	CCSD(T)/6-311G(d,p)	12.0
	CCSD(T)/6-311++G(2df,2p)	11.5

<sup>a</sup> Relative energies are reported in kcal mol<sup>-1</sup>.

motion of the H' bonded to the ion, respectively. For Cl<sup>-</sup>·H<sub>2</sub>O, we see the uncomplexed OH stretch occurring at 3785 cm<sup>-1</sup>. This value is in excellent agreement with 3698 cm<sup>-1</sup>, reported by Choi et al.<sup>18</sup> Also, our calculated OH complexed stretch is predicted to occur at 3524 cm<sup>-1</sup>. This compares with the experimental value of 3285 cm<sup>-1</sup> for the complexed OH stretch<sup>18</sup> and the experimental value of 3103 cm<sup>-1</sup> from argon predissociation spectroscopy stretches.<sup>21</sup>

The relative energies for Cl<sup>-</sup>·H<sub>2</sub>O are included in Table 3. Again, our best estimate of the binding energy of this complex is determined at the CCSD(T)/6-311++G(2df,2p) level of theory. At this level of theory, we find the complex to be bound by 14.1 kcal mol<sup>-1</sup>. This value compares very well with the previously calculated values of 13.61 kcal mol<sup>-1</sup>, as well as 12.9 and 17.2 kcal mol<sup>-1</sup>.<sup>22,23</sup> When compared with experimental results,<sup>24,25</sup> our value of 14.1 kcal mol<sup>-1</sup> is in excellent agreement with the experimental determinations of 14.3 and 14.8 kcal mol<sup>-1</sup>. This indicates that our computational method

provides reasonable and reliable results. Moreover, they are good systems for calibrating the calculations on  $\text{Cl}^- \cdot \text{HOBr}$  and  $\text{Br}^- \cdot \text{HOCl}$  species for which no experimental results are available.

For  $\text{Br}^- \cdot \text{H}_2\text{O}$ , we also report the fully optimized molecular geometries in Table 1. Again, we have used the  $C_s$  structure, which is of minimum energy. Our best estimation for the equilibrium geometry parameters occurs again at the CCSD(T)/6-311++G(2df,2p) level of theory. We note that all parameters have converged to this level. At this level, we report an X–H–O angle of  $164.3^\circ$ . This value agrees well with the  $165^\circ$  value reported by Xantheas,<sup>20</sup> using MP2/MP4(aug-cc-pVDZ/aug-cc-pVTZ) basis sets. Also, our calculated value for the H'O bond only differs by 0.006 Å when compared to Xantheas' result. We note here, as well, similar trends in shortening the H'O bond. We observe the H'O bond in  $\text{Cl}^- \cdot \text{H}_2\text{O}$  to be 0.985 Å, and the H'O bond for  $\text{Br}^- \cdot \text{H}_2\text{O}$  to be 0.979 Å, both at the CCSD(T)/6-311++G(2df,2p) level of theory. Xantheas<sup>20</sup> noted a similar trend with MP2/MP4(aug-cc-pVDZ/aug-cc-pVTZ) calculations (H'O = 0.992 and 0.987 Å for  $\text{Cl}^- \cdot \text{H}_2\text{O}$  and  $\text{Br}^- \cdot \text{H}_2\text{O}$ , respectively).

The harmonic vibrational frequencies for  $\text{Br}^- \cdot \text{H}_2\text{O}$  have been calculated and are shown in Table 2. Again, we see six normal vibrational modes. These normal modes are represented by  $\nu_1$  and  $\nu_2$  for uncomplexed (OH) and complexed (H'O) stretches, respectively. The H'OH bend is  $\nu_3$ , while the  $\text{H}_2\text{O}$  in-plane rock with respect to  $\text{Br}^-$  is represented by  $\nu_4$ .  $\nu_5$  is the van der Waals stretch motion for the  $\text{Br}-\text{H}'$ , and  $\nu_6$  is the out-of-plane motion of the hydrogen bonded to the  $\text{Br}^-$ . We note that all frequencies presented have real, positive values, which indicates that the structure is a true minimum on the potential energy surface. We report frequencies at the CCSD(T)/6-311G(d,p) level. At this level of computation, we find the uncomplexed OH stretch ( $\nu_1$ ) to occur at  $3945 \text{ cm}^{-1}$ . We see good agreement between the calculated and experimental<sup>26</sup> frequency for the OH stretch occurring in  $\text{H}_2\text{O}$  at  $3943 \text{ cm}^{-1}$ . Also, the complexed H'O stretch is estimated to occur at  $3565 \text{ cm}^{-1}$ . This is in good agreement with experimentally determined vibrational frequencies established by Ayotte et al.<sup>27</sup> They report a complexed H'O stretch occurring in  $\text{Br}^- \cdot \text{H}_2\text{O}$  at  $3368 \pm 3 \text{ cm}^{-1}$ .

We have also calculated the relative binding energies for  $\text{Br}^- \cdot \text{H}_2\text{O}$ . These results are included in Table 3. The binding energy has converged to give our best estimation at the CCSD(T)/6-311++G(2df,2p) level. Here we predict that the  $\text{Br}^- \cdot \text{H}_2\text{O}$  complex is bound by  $11.5 \text{ kcal mol}^{-1}$ . This is in excellent agreement with the experimental<sup>26</sup> value of  $12.3 \text{ kcal mol}^{-1}$ .

**B.  $\text{Cl}^- \cdot \text{HOBr}$  vs  $\text{Cl}^- \cdot \text{BrOH}$ .** A primary goal of this study is to determine the equilibrium geometry of the chlorine anion as it binds to hypobromous acid (HOBr). To accomplish this, we have used two possible conformers of the complex. The first form places the chlorine anion in complexation through the hydrogen of HOBr. The second conformer considered places the chlorine anion in complexation through the bromine of HOBr. The geometries are given in Table 4. In the first conformation,  $\text{Cl}^- \cdot \text{HOBr}$ , we see interesting effects when compared to the geometry of  $\text{Cl}^- \cdot \text{H}_2\text{O}$ , primarily the shortening of the  $\text{Cl}-\text{H}'$  bond. This length decreases by 0.22 Å relative to  $\text{Cl}^- \cdot \text{H}_2\text{O}$ , indicating that the chlorine is more strongly bound to HOBr than to  $\text{H}_2\text{O}$ . Also, there is a relatively small lengthening of the H'O bond in  $\text{Cl}^- \cdot \text{HOBr}$  relative to uncomplexed HOBr. This bond length has increased by 0.052 Å, which indicates that the chlorine complexation has little effect on the bonds in HOBr. This is further evidenced when examining the HOBr angle in  $\text{Cl}^- \cdot \text{HOBr}$  relative to uncomplexed HOBr. At

the CCSD(T)/6-311++G(2df,2p) level, the HOBr angle only changes by  $1^\circ$  upon chlorine complexation.

For the other conformation,  $\text{Cl}^- \cdot \text{BrOH}$ , we see subtle effects due to chlorine complexation through the bromine of HOBr. First we note that, at the CCSD(T)/6-311++G(2df,2p) level, the HOBr angle in  $\text{Cl}^- \cdot \text{BrOH}$  closes by  $2.8^\circ$  relative to uncomplexed HOBr and by  $3.8^\circ$  relative to  $\text{Cl}^- \cdot \text{HOBr}$ . This results in a closer arrangement of the atoms in the complex. However, when comparing the geometry of HOBr and  $\text{Cl}^- \cdot \text{HOBr}$ , one observes a small HOBr geometry distortion after chlorine complexation. In uncomplexed HOBr at the CCSD(T)/6-311++G(2df,2p) level, we see an OH bond length of 0.964 Å and a BrO bond length of 1.84 Å. In  $\text{Cl}^- \cdot \text{HOBr}$  at the CCSD(T)/6-311++G(2df,2p) level, we see an OH bond length of 0.962 Å and a BrO bond length of 1.982 Å. Thus, the BrO bond in  $\text{Cl}^- \cdot \text{BrOH}$  is only 0.143 Å longer than in HOBr.

The vibrational frequencies for both  $\text{Cl}^- \cdot \text{HOBr}$  and  $\text{Cl}^- \cdot \text{BrOH}$  are included in Table 5. We report all frequencies are positive real numbers, which indicates that the geometry is a true minimum structure on the potential energy surface. For the OH stretch in  $\text{Cl}^- \cdot \text{HOBr}$ , we report a value of  $3026 \text{ cm}^{-1}$ . This corresponds well to the HO stretch occurring in isolated HOBr, at  $3838 \text{ cm}^{-1}$  (experimental<sup>28</sup>  $3590 \text{ cm}^{-1}$ ). This red shift of  $812 \text{ cm}^{-1}$  is reasonable when inspecting the HO bond length in HOBr and  $\text{Cl}^- \cdot \text{HOBr}$ . At the CCSD(T)/6-311++G(2df,2p) level, we calculate an HO bond length of 0.964 Å, while in  $\text{Cl}^- \cdot \text{HOBr}$ , the HO bond length was calculated to be 1.016 Å. The longer HO bond suggests that the frequency of this motion should be red shifted. Also, the HO stretch in  $\text{Cl}^- \cdot \text{HOBr}$  is in agreement with the complexed HO stretch in  $\text{Cl}^- \cdot \text{H}_2\text{O}$ . Our CCSD(T) result is close to the  $3285 \text{ cm}^{-1}$  reported by Choi et al.<sup>18</sup> Upon further inspection, we see the HO bond length in  $\text{Cl}^- \cdot \text{H}_2\text{O}$  to be 0.985 Å at the CCSD(T)/6-311++G(2df,2p) level. This value is 0.031 Å shorter than our calculation for the HO bond in  $\text{Cl}^- \cdot \text{HOBr}$ . Thus, we see that, as the calculated HO bond length increases through the series HOBr,  $\text{Cl}^- \cdot \text{H}_2\text{O}$ , and  $\text{Cl}^- \cdot \text{HOBr}$ , the HO stretching frequency decreases through the same series. The HOBr bending mode is also affected by the chlorine complexation. We noted previously that chlorine complexation through the hydrogen affected the geometry of the HOBr monomer. This effect is also seen in the HOBr bending frequency. The lengthening of the HO bond by 0.052 Å, as well as the closing of the HOBr angle by  $1^\circ$  (both of which are results of the  $\text{Cl}^-$  complexation), causes the HOBr bending frequency to be blue shifted. Also, the BrO stretching frequency in  $\text{Cl}^- \cdot \text{HOBr}$  is in good agreement with the experimental BrO stretching frequency from HOBr. We estimate a BrO stretch to occur in  $\text{Cl}^- \cdot \text{HOBr}$  at  $575 \text{ cm}^{-1}$ , which is relatively similar to the experimental BrO stretch of  $626 \text{ cm}^{-1}$ .<sup>28</sup> We also predict the  $\text{Cl}^- \cdot \text{H}$  stretch to occur at  $259 \text{ cm}^{-1}$ .

For  $\text{Cl}^- \cdot \text{BrOH}$ , from our CCSD(T)/6-311G(d,p) calculations in Table 5, we report an OH stretching frequency of  $3822 \text{ cm}^{-1}$ . This is red shifted by  $16 \text{ cm}^{-1}$  from the OH stretch. Here, we see that the  $\text{Cl}^-$  complexation has little effect on the HOBr bending frequency. We calculate an HOBr bending frequency of  $1016 \text{ cm}^{-1}$ , which is in excellent agreement with the calculated and experimental HOBr bend<sup>21</sup> of  $1164 \text{ cm}^{-1}$ . The largest difference in bond lengths in  $\text{Cl}^- \cdot \text{BrOH}$  relative to HOBr is the elongation of the BrO bond. In HOBr, we report a BrO bond length of 1.84 Å, while in  $\text{Cl}^- \cdot \text{BrOH}$ , we report a BrO bond length of 1.98 Å. This effect is also seen in the BrO stretching frequency, namely the BrO stretch, which decreases from  $575 \text{ cm}^{-1}$  (HOBr) to  $435 \text{ cm}^{-1}$  ( $\text{Cl}^- \cdot \text{BrOH}$ ). The elonga-

**TABLE 4: Geometries<sup>a</sup> for  $\text{Cl}^- \cdot \text{HOBr}$ ,  $\text{Cl}^- \cdot \text{BrOH}$ ,  $\text{Br}^- \cdot \text{HOCl}$ ,  $\text{Br}^- \cdot \text{ClOH}$ ,  $\text{Br}^- \cdot \text{HOBr}$ , and  $\text{Br}^- \cdot \text{BrOH}$** 

species	level of theory	geometric parameters				
		$r(\text{Cl-X})$	$r(\text{OH})$	$r(\text{BrO})$	$\theta(\text{Cl-XO})$	$\theta(\text{HOBr})$
$\text{Cl}^- \cdot \text{HOBr}$ X = H	MP2/6-31G(d)	1.951	1.027	1.849	175.9	102.3
	MP2/6-311G(d,p)	1.914	1.013	1.844	176.1	102.7
	MP2/6-311++G(2df,2p)	1.864	1.026	1.804	176.6	103.8
	CCSD(T)/6-31G(d)	1.980	1.022	1.873	175.6	102.1
	CCSD(T)/6-311G(d,p)	1.939	1.008	1.868	175.5	102.5
$\text{Cl}^- \cdot \text{BrOH}$ X = Br	CCSD(T)/6-311++G(2df,2p)	1.912	1.016	1.824	176.2	103.9
	MP2/6-31G(d)	2.603	0.980	1.994	179.6	102.2
	MP2/6-311G(d,p)	2.660	0.962	1.980	179.1	97.8
	MP2/6-311++G(2df,2p)	2.516	0.963	1.991	179.6	99.2
	CCSD(T)/6-31G(d)	2.647	0.976	2.003	179.5	98.5
$\text{Br}^- \cdot \text{HOCl}$ X = H	CCSD(T)/6-311G(d,p)	2.713	0.962	1.982	179.0	98.6
	CCSD(T)/6-311++G(2df,2p)	2.582	0.962	1.983	179.7	100.1
	MP2/6-31G(d)	2.134	1.019	1.797	178.0	103.1
	MP2/6-311G(d,p)	2.110	1.003	1.710	176.5	102.9
	MP2/6-311++G(2df,2p)	2.079	1.010	1.680	176.3	103.6
$\text{Br}^- \cdot \text{ClOH}$ X = Br	CCSD(T)/6-31G(d)	2.170	1.015	1.730	177.1	102.8
	CCSD(T)/6-311G(d,p)	2.138	1.000	1.735	175.4	102.5
	CCSD(T)/6-311++G(2df,2p)	2.130	1.004	1.699	175.2	103.5
	MP2/6-31G(d)	2.768	0.976	1.831	178	99.2
	MP2/6-311G(d,p)	2.792	0.963	1.840	178.6	98.1
$\text{Br}^- \cdot \text{HOBr}$ X = H	MP2/6-311++G(2df,2p)	2.576	0.964	1.876	180.0	97.6
	CCSD(T)/6-31G(d)	2.844	0.977	1.830	178.5	99.8
	CCSD(T)/6-311G(d,p)	2.901	0.962	1.831	178.0	98.9
	CCSD(T)/6-311++G(2df,2p)	2.725	0.962	1.833	179.6	99.2
	$\text{Br}^- \cdot \text{BrOH}$ X = Br	MP2/6-31G(d)	2.115	1.021	1.850	180.0
MP2/6-311G(d,p)		2.115	1.003	1.846	176.6	102.3
MP2/6-311++G(2df,2p)		2.074	0.963	1.991	176.8	98.9
CCSD(T)/6-31G(d)		2.155	1.016	1.874	179.0	101.6
CCSD(T)/6-311G(d,p)		2.151	0.998	1.869	175.8	102.1
$\text{Br}^- \cdot \text{BrOH}$ X = Br	CCSD(T)/6-311++G(2df,2p)	2.127	1.004	1.827	176.3	103.6
	MP2/6-31G(d)	2.711	0.976	2.001	179.5	97.8
	MP2/6-311G(d,p)	2.775	0.963	1.992	179.1	97.3
	MP2/6-311++G(2df,2p)	2.680	0.964	1.991	179.7	98.9
	CCSD(T)/6-31G(d)	2.755	0.977	2.012	179.4	98.3
$\text{Br}^- \cdot \text{BrOH}$ X = Br	CCSD(T)/6-311G(d,p)	2.838	0.962	1.993	178.9	98.3
	CCSD(T)/6-311++G(2df,2p)	2.706	0.962	1.977	179.8	100.0

<sup>a</sup> All bond distances are reported in angstroms and bond angles in degrees.

tion of the BrO bond by 0.14 Å induces a BrO stretching red shift of 140  $\text{cm}^{-1}$ .

The total energies for  $\text{Cl}^- \cdot \text{HOBr}$  and  $\text{Cl}^- \cdot \text{BrOH}$  anionic clusters are given in Table 6. In Table 7, we report the zero-point energy corrected binding energies of the complexes, as well as the relative energies between  $\text{Cl}^- \cdot \text{HOBr}$  and  $\text{Cl}^- \cdot \text{BrOH}$ . We find the  $\text{Cl}^- \cdot \text{HOBr}$  structure to be the lowest in energy. At the CCSD(T)/6-311++G(2df,2p) level, we calculate  $\text{Cl}^- \cdot \text{HOBr}$  to be lower in energy by 1.5  $\text{kcal mol}^{-1}$ . We also estimate the binding energies of both complexes. We find the  $\text{Cl}^- \cdot \text{HOBr}$  complex to be bound by 23.0  $\text{kcal mol}^{-1}$  and  $\text{Cl}^- \cdot \text{BrOH}$  to be bound by 21.5  $\text{kcal mol}^{-1}$ . These energetic calculations suggest that, if the heterogeneous reaction mechanism proposed by Chu and Chu<sup>11</sup> exists, the  $\text{Cl}^-[\text{HOBr}]$  intermediate is likely to be of the form  $\text{Cl}^- \cdot \text{HOBr}$ .

**C.  $\text{Br}^- \cdot \text{HOCl}$  vs  $\text{Br}^- \cdot \text{ClOH}$ .** Like the  $\text{Cl}^- \cdot \text{HOBr}$  system, the  $\text{Br}^- \cdot \text{HOCl}$  system has two conformers. The first conformer takes the form of the bromine anion complexing to the HOCl through the hydrogen, whereas in the second conformation, the bromine anion is in complexation through the chlorine of HOCl. A complete list of fully optimized geometrical parameters for both conformations comprises Table 4. For the first conforma-

tion of  $\text{Br}^-$  bound through the hydrogen, a comparison with previous calibration calculations for the  $\text{Br}^- \cdot \text{H}_2\text{O}$  system yields some interesting results. We first note that there is a significant shortening of the  $\text{Br}^- - \text{H}$  bond in  $\text{Br}^- \cdot \text{H}_2\text{O}$ . This bond length was further reduced by 0.237 Å, indicating that the  $\text{Br}^- - \text{H}$  bond in  $\text{Br}^- \cdot \text{HOCl}$  is stronger than that in  $\text{Br}^- \cdot \text{H}_2\text{O}$ . Also, the  $\text{Br}^- - \text{HO}$  angle in  $\text{Br}^- \cdot \text{HOCl}$  increases by 10.9° relative to  $\text{Br}^- \cdot \text{H}_2\text{O}$ . This result also indicates that the  $\text{Br}^-$  is more tightly bound in  $\text{Br}^- \cdot \text{HOCl}$  than in  $\text{Br}^- \cdot \text{H}_2\text{O}$ . We see that the HO bond length in  $\text{Br}^- \cdot \text{HOCl}$  is 0.015 Å longer than for HOCl, indicating that the bromine complexation exhibits a marginal effect on the HO bonding.

For the  $\text{Br}^- \cdot \text{ClOH}$  conformer, we see the most effect on the HOCl angle. At the CCSD(T)/6-311++G(2df,2p) level, the HOCl angle in HOCl is 102.4°. However, in  $\text{Br}^- \cdot \text{ClOH}$ , the angle closes to 99.2°. From this, we see that, in this conformation, the ClOH geometry is more constrained in  $\text{Br}^- \cdot \text{ClOH}$  than for HOCl. Also, the ClO bond is affected by the bromine complexation. In HOCl, we calculate a ClO bond length of 1.707 Å. This ClO distance increases upon bromine complexation through chlorine to 1.833 Å. These factors indicate that the

**TABLE 5: Vibrational Frequencies (in  $\text{cm}^{-1}$ ) for  $\text{Cl}^- \cdot \text{HOBr}$ ,  $\text{Cl}^- \cdot \text{BrOH}$ ,  $\text{Br}^- \cdot \text{HOCl}$ ,  $\text{Br}^- \cdot \text{ClOH}$ ,  $\text{Br}^- \cdot \text{HOBr}$ , and  $\text{Br}^- \cdot \text{BrOH}$  Anion Clusters<sup>a</sup>**

species	mode no.	mode symmetry	mode description	CCSD(T)/6-311G(d,p)
HOCl	1	$a'$	HO stretch	3840
	2		HOCl bend	1219
	3		ClO stretch	664
HOBr	1	$a'$	HO stretch	3838
	2		HOBr bend	1164
	3		BrO stretch	575
$\text{Cl}^- \cdot \text{HOBr}$	1	$a'$	HO stretch	3026
	2		HOBr bend	1408
	3		BrO stretch	829
	4		Cl-H stretch	574
	5		HOBr in-plane rock	259
	6		out-of-plane motion of H bonded to the ion	88
$\text{Cl}^- \cdot \text{BrOH}$	1	$a'$	HO stretch	3822
	2		HOBr bend	1016
	3		BrO stretch	435
	4		Cl-Br stretch	165
	5		HOBr in-plane rock	157
	6		out-of-plane motion of Cl ion bonded to BrOH	150
$\text{Br}^- \cdot \text{HOCl}$	1	$a'$	HO stretch	3184
	2		HOCl bend	1405
	3		ClO stretch	659
	4		$\text{Br}^-$ -H stretch	747
	5		HOCl in-plane rock	216
	6		out-of-plane motion of the H bonded to the ion	83
$\text{Br}^- \cdot \text{ClOH}$	1	$a'$	HO stretch	3848
	2		HOCl bend	1094
	3		ClO stretch	479
	4		HOCl in-plane rock	144
	5		$\text{Br}^-$ -Cl stretch	105
	6		out-of-plane motion of the H bonded to the ion	158
$\text{Br}^- \cdot \text{HOBr}$	1	$a'$	HO stretch	3202
	2		HOBr bend	1361
	3		BrO stretch	731
	4		Br-H stretch	575
	5		HOBr in-plane rock	208
	6		out-of-plane motion of the H bonded to the ion	64
$\text{Br}^- \cdot \text{BrOH}$	1	$a'$	HO stretch	3845
	2		HOBr bend	1016
	3		BrO stretch	439
	4		Br-Br stretch	144
	5		HOBr in-plane rock	135
	6		out-of-plane motion of the H bonded to the ion	123

<sup>a</sup> Experimental frequencies for HOBr: 3590, 1164, and  $626 \text{ cm}^{-1}$ . Experimental frequencies for HOCl: 3581, 1239, and  $718 \text{ cm}^{-1}$ , taken from ref 26. Experimental frequencies for HOBr: 3590, 1164, and  $626 \text{ cm}^{-1}$ , taken from ref 26.

**TABLE 6: Total Energies for Anion Clusters and Monomers<sup>a</sup>**

level of theory	$\text{Cl}^- \cdot \text{HOBr}$	$\text{Cl}^- \cdot \text{BrOH}$	HOBr	$\text{Cl}^-$	$\text{Br}^- \cdot \text{HOCl}$	$\text{Br}^- \cdot \text{ClOH}$	HOCl	$\text{Br}^-$	$\text{Br}^- \cdot \text{HOBr}$	$\text{Br}^- \cdot \text{BrOH}$
MP2/6-31G(d)	-3105.29210	-3105.28813	-2645.58910	-459.66182	-3105.28904	-3105.27155	-535.16944	-2570.07908	-5215.70922	-5215.70956
MP2/6-311G(d,p)	-3108.29790	-3108.29025	-2648.51368	-459.74884	-3108.29122	-3108.27443	-535.30317	-2572.95404	-5221.50046	-5221.49653
MP2/6-311++G(2df,2p)	-3108.48682	-3108.48366	-2648.62514	-459.82115	-3108.48216	-3108.46861	-535.42487	-2573.02273	-5221.68220	-5221.68077
CCSD(T)/6-31G(d)	-3105.28860	-3105.28366	-2645.58212	-459.66654	-3105.28606	-3105.26777	-535.18356	-2570.06349	-5215.68481	-5215.68335
CCSD(T)/6-311G(d,p)	-3107.87540	-3107.86697	-2648.12635	-459.71447	-3107.86878	-3107.85116	-535.26337	-2572.57231	-5220.73024	-5220.72500
CCSD(T)/6-311++G(2df,2p)	-3108.03977	-3108.03458	-2648.21882	-459.78220	-3108.03610	-3108.02001	-535.37775	-2572.62575	-5220.87690	-5220.87297

<sup>a</sup> Total energies are in Hartrees.

bromine through chlorine complexation distorts HOCl more than does bromine through hydrogen complexation.

We report the harmonic vibrational frequencies for both conformers in Table 5. Many of the structural charges noted above are manifested in the shifts in the vibrational frequencies compared to the HOCl monomer. From comparison with the vibrational modes of HOCl, we see there are significant frequency shifts due to bromine complexation. At the CCSD(T)/6-311G(d,p) level, we calculate the HO stretch in  $\text{Br}^- \cdot \text{HOCl}$  to occur at  $3184 \text{ cm}^{-1}$ . This is red shifted by  $656 \text{ cm}^{-1}$  from the HO stretch in HOCl<sup>28</sup> ( $3840 \text{ cm}^{-1}$ ). The red shift here is consistent with the elongation of the HO bond due to complexation. At the CCSD(T)/6-311++G(2df,2p) level, we report an

HO bond distance of  $1.004 \text{ \AA}$  for  $\text{Br}^- \cdot \text{HOCl}$ , but only  $0.964 \text{ \AA}$  for the HO bond in HOCl. The longer HO bond vibrates at a lower frequency. The HOCl bending mode ( $\nu_2$ ) is blue shifted by  $186 \text{ cm}^{-1}$ . This blue shift is in response to the opening of the HOCl angle by bromine complexation. The HOCl angle is opened by  $1.1^\circ$ , which allows the HOCl bend to occur at higher frequency. For the  $\text{Br}^- \cdot \text{ClOH}$  conformation, we see similar effects in the calculated frequency results.

The calculated total energies for the  $\text{Br}^- \cdot \text{HOCl}$  and  $\text{Br}^- \cdot \text{ClOH}$  complexes are listed in Table 6. Also, the binding energies, which contain a zero-point correction, are included in Table 7. We see that the results have converged to give our best estimation of the energetics of these complexes at the CCSD-

**TABLE 7: Relative Energies<sup>a</sup> for Cl<sup>-</sup>·HOBr, Cl<sup>-</sup>·BrOH, Br<sup>-</sup>·HOCl, Br<sup>-</sup>·ClOH, Br<sup>-</sup>·HOBr, and Br<sup>-</sup>·BrOH Anion Clusters**

level of theory	Cl <sup>-</sup> ·HOBr		Cl <sup>-</sup> ·BrOH	Br <sup>-</sup> ·HOCl		Br <sup>-</sup> ·ClOH	Br <sup>-</sup> ·HOBr		Br <sup>-</sup> ·BrOH
	Cl <sup>-</sup> ·BrOH	Cl <sup>-</sup> + HOBr	Cl <sup>-</sup> + HOBr	Br <sup>-</sup> ·ClOH	Br <sup>-</sup> + HOCl	Br <sup>-</sup> + HOCl	Br <sup>-</sup> ·BrOH	Br <sup>-</sup> + HOBr	Br <sup>-</sup> + HOBr
MP2/6-31G(d)	2.5	25.8	23.3	11.0	25.4	14.4	-0.2	25.8	26.0
MP2/6-311G(d,p)	4.8	22.2	17.4	10.5	21.4	10.9	2.5	20.6	18.1
MP2/6-311++G(2df,2p)	2.0	25.4	23.4	8.5	21.7	13.3	0.9	21.6	20.7
CCSD(T)/6-31G(d)	3.1	25.1	22.0	11.5	24.5	13.0	0.9	24.6	23.7
CCSD(T)/6-311G(d,p)	5.3	21.7	16.4	11.1	20.7	9.6	3.3	19.8	16.5
CCSD(T)/6-311++G(2df,2p)	3.3	24.3	21.0	10.1	20.5	10.4	2.5	20.3	17.8
ΔZPE	-0.7	-1.0	-0.3	-0.7	-1.0	-0.3	-0.7	-0.8	-0.1
CCSD(T)/6-311++G(2df,2p) + ΔZPE	2.6	23.3	20.7	9.4	19.5	10.1	1.8	19.5	17.7

<sup>a</sup> Relative energies are reported in kcal mol<sup>-1</sup>.

**TABLE 8: Total Energies and Acidity of H·X (X = Cl, Br, OH, ClO, BrO)**

species	MP2			CCSD(T)			exp
	6-31G(d)	6-311G(d,p)	6-311++G(2df,2p)	6-31G(d)	6-311G(d,p)	6-311++G(2df,2p)	
Experimental Total Energies (Hartree)							
Cl <sup>-</sup>	-459.66182	-459.74884	-459.82115	-459.66654	-459.71447	-459.78220	
Br <sup>-</sup>	-2570.07908	-2572.95404	-2573.02273	-2570.06349	-2572.57231	-2572.62575	
HCl	-460.20215	-460.29297	-460.35776	-460.21159	-460.26332	-460.32251	
HBr	-2570.60758	-2573.48429	-2573.54019	-2570.59760	-2573.10791	-2573.14673	
OH <sup>-</sup>	-75.51544	-75.59231	-75.70340	-75.52183	-75.58284	-75.68952	
ClO <sup>-</sup>	-534.56623	-534.69131	-534.84610	-534.58066	-534.65186	-534.79552	
BrO <sup>-</sup>	-2644.99033	-2647.90248	-2648.04766	-2644.98346	-2647.51481	-2647.63831	
H <sub>2</sub> O	-76.19924	-76.28290	-76.33617	-76.20785	-76.27619	-76.32827	
HOCl	-535.16944	-535.30317	-535.42487	-535.18356	-535.26337	-535.37775	
HOBr	-2645.58910	-2648.51368	-2648.62514	-2645.58212	-2648.12635	-2648.21882	
Acidity <sup>a</sup> (kcal mol <sup>-1</sup> )							
HCl → H <sup>+</sup> + Cl <sup>-</sup>	334.8	337.1	332.4	337.7	340.1	334.7	328.1
HBr → H <sup>+</sup> + Br <sup>-</sup>	327.8	328.9	320.9	331.3	336.1	323.1	318.3
HOH → H <sup>+</sup> + OH <sup>-</sup>	420.7	425.0	388.7	422.1	383.4	392.4	384.1
HOCl → H <sup>+</sup> + ClO <sup>-</sup>	371.1	376.5	355.8	370.9	376.3	358.0	349.2
HOBr → H <sup>+</sup> + BrO <sup>-</sup>	368.4	376.2	355.0	368.4	376.4	357.0	347.1

<sup>a</sup> Corrected for CCSD(T)/6-311G(d,p) zero-point energy.

(T)/6-311++G(2df,2p) level of computation. At this level, we find Br<sup>-</sup>·HOCl to be the lowest energy conformation. From these results, we see that Br<sup>-</sup>·HOCl is bound by 19.5 kcal mol<sup>-1</sup>, whereas the Br<sup>-</sup>·ClOH conformation is bound by 10.1 kcal mol<sup>-1</sup>. We see that the Br<sup>-</sup>·HOCl conformation is lower in energy by 9.4 kcal mol<sup>-1</sup> relative to Br<sup>-</sup>·ClOH. Again, based upon the mechanism proposed by Chu and Chu,<sup>11</sup> the intermediate would most likely exist in the form Br<sup>-</sup>·HOCl.

It is interesting to compare the Cl<sup>-</sup>·BrOH with Br<sup>-</sup>·ClOH. These anions are isoelectronic with the triatomic halide anions: Cl<sup>-</sup>·BrF and Br<sup>-</sup>·ClF. In heteronuclear trihalide anions, the heaviest halide tends to occupy the central anion position.<sup>30</sup> A recent study of heteronuclear trihalide anions involving chlorine, bromine, and iodine has confirmed that isomers in which the heaviest atom occupies the central position are more stable than those in which the lighter atom occupies the central position.<sup>31</sup> In the case of Cl<sup>-</sup>·BrOH and Br<sup>-</sup>·ClOH, the Cl<sup>-</sup>·BrOH is more stable by 9.3 kcal mol<sup>-1</sup> at the CCSD(T)/6-311++G(2df,2p) level of theory. This is consistent with energy differences for Cl<sup>-</sup>·BrCl and Br<sup>-</sup>·ClCl of 10.6 kcal mol<sup>-1</sup> and Br<sup>-</sup>·BrCl and Br<sup>-</sup>·ClBr of 9.4 kcal mol<sup>-1</sup> at the MP3/MID-4\*/MP2/MIDI-4\*+ level of theory.<sup>31</sup>

**D. Br<sup>-</sup>·HOBr vs Br<sup>-</sup>·BrOH.** The species of interest in this study is the complex formed between bromine anions and hypobromous acid. Again, we have considered two possible conformers, the first with the bromine anion complexing through the hydrogen of HOBr and the second with the bromine anion complexing through the bromine atom of HOBr. We report fully optimized geometries at all levels of calculation in Table 4 for this system and, accordingly, our best estimate as to the equilibrium geometry of these complexes occurs at the CCSD(T)/6-311++G(2df,2p) level of calculation. When comparing

the geometries of these complexes, we also include the Br<sup>-</sup>·H<sub>2</sub>O geometry optimizations as another point of comparison. In the case of Br<sup>-</sup>·HOBr, we see a shortening of the Br–H bond relative to Br<sup>-</sup>·H<sub>2</sub>O. Our CCSD(T)/6-311++G(2df,2p) result estimates this bond to be about 0.2 Å shorter in Br<sup>-</sup>·HOBr than in Br<sup>-</sup>·H<sub>2</sub>O. This indicates that the bromine anion is more strongly bound to HOBr than to H<sub>2</sub>O. Also, we note a lengthening of the HO bond due to bromine complexation. In Br<sup>-</sup>·H<sub>2</sub>O, the H'O bond length is 0.979 Å, whereas in Br<sup>-</sup>·HOBr, the H'O bond length is predicted to be 1.00 Å at the CCSD(T)/6-311++G(2df,2p) level. Another interesting effect of the bromine complexation is the opening of the HOBr angle relative to uncomplexed HOBr. At the CCSD(T)/6-311++G(2df,2p) level, we calculate the HOBr angle in HOBr to be 102.9°, whereas this angle opens up to 103.6° in Br<sup>-</sup>·HOBr. This 0.7° opening is due to the additional repulsion added by the complexation of the bromine atom.

For the Br<sup>-</sup>·BrOH case, we also note some more subtle effects of the bromine complexation through the bromine of HOBr. First, we see that the Br–Br bond is predicted to be 2.706 Å at the CCSD(T)/6-311++G(2df,2p) level. Complexation through the hydrogen of HOBr also opened the HOBr bond angle relative to complexation through the bromine. At the CCSD(T)/6-311++G(2df,2p) level, we see the HOBr bond angle open from 100.0° in Br<sup>-</sup>·BrOH to 103.6° in Br<sup>-</sup>·HOBr.

Our frequency calculations in Table 5 are reported at the CCSD(T)/6-311G(d,p) level of theory. At this level, we report the HO stretch in Br<sup>-</sup>·HOBr to be red shifted by 633 cm<sup>-1</sup>. This can be explained by the lengthening of the OH bond in Br<sup>-</sup>·HOBr relative to uncomplexed HOBr. The OH bond is 0.04 Å longer; thus, the bond stretches at the red shifted frequency.

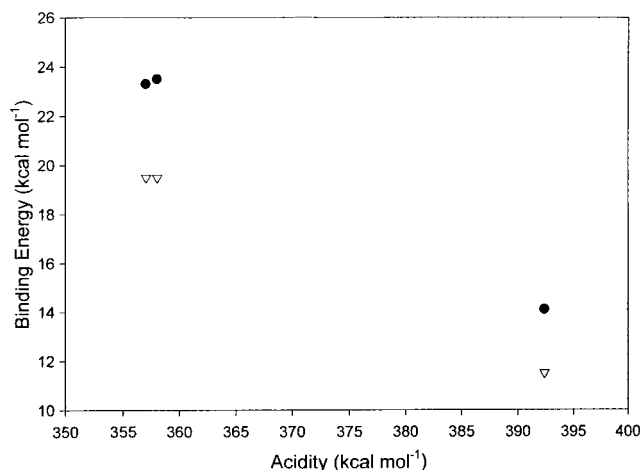


**Figure 1.** Plot of  $X^- \cdot HOY$  (where  $X = Cl$  or  $Br$  and  $Y = H, Cl, Br$ ) binding energy versus acidity of the  $HOY$  monomer. Closed circle represents  $Cl^- \cdot HOY$  and open triangle represents  $Br^- \cdot HOY$ .

Tables 6 and 7 contain the results of the energetic studies for these conformers. At the CCSD(T)/6-311++G(2df,2p) level of theory, the trends in the relative energetics of these complexes show that the lowest energy structure of the two conformers places the halogen in complexation through the hydrogen of the acid. We also find that  $Br^- \cdot BrOH$  is stable to dissociation into  $Br^-$  and  $HOBr$  by  $17.7 \text{ kcal mol}^{-1}$ . As well, we note that  $Br^- \cdot HOBr$  is stable to the same dissociation pathway by  $19.5 \text{ kcal mol}^{-1}$ . There is a  $1.8 \text{ kcal mol}^{-1}$  difference in energy between  $Br^- \cdot BrOH$  and  $Br^- \cdot HOBr$ . These results are quite interesting. In solution,<sup>17,29</sup> the reaction of  $HOBr$  with ionized  $HBr$



is consistent with the involvement of a  $Br^- \cdot BrOH$  intermediate which, upon attack of  $H^+$ , yields the products  $Br_2 + H_2O$ , viz.



It could be the case that the energy of solvation may drive the  $Br^- + HOBr$  reaction toward the  $Br^- \cdot BrOH$  instead of the  $Br^- \cdot HOBr$  intermediate.

To better understand the strength of the  $X^- \cdot HOY$  (where  $X, Y = H, Cl, \text{ or } Br$ ) bond, we have calculated the acidities for  $HOY$ . The calculated acidities are reported in Table 8. A comparison of the calculated acidities with experimental known values show that the rms error between the values is  $8.8 \text{ kcal mol}^{-1}$  at the CCSD(T)/6-311++G(2df,2p) level of theory. Nevertheless, the calculated acidities follow the same trend as the experimental reported values. As shown in Figure 1, there is a trend in the binding energies of the complex with the acidity for both chlorine and bromine anions. The data suggest that the more acidic the hydrogen, the more likely that the halogen anion will be tightly bound to the  $HOX$ . The data also indicate that the binding energies for  $X^- \cdot HOCl$  and  $X^- \cdot HOBr$ , where  $X = Cl$  and  $Br$ , are very close in energy because the acidities of  $HOCl$  and  $HOBr$  are close in value. Indeed, the calculations from Table 7 suggest that these binding energies are close in energy.

#### IV. Conclusions

Ab initio molecular orbital calculations have been employed to probe the molecular geometries, vibrational frequencies, and energetics of  $Cl^- \cdot HOBr$ ,  $Cl^- \cdot BrOH$ ,  $Br^- \cdot HOCl$ ,  $Br^- \cdot ClOH$ ,  $Br^- \cdot HOBr$ , and  $Br^- \cdot HOBr$  anionic complexes. For the  $Cl^- \cdot HOBr$  complexes, we predict that  $Cl^-$  would most likely be bound to the hydrogen of  $HOBr$ . The binding energy of this structure is predicted to be  $23.2 \text{ kcal mol}^{-1}$ . For the  $Br^- \cdot HOCl$  type complexes, we find that the  $Br^-$  most likely complexes through the hydrogen, as well. This complex is bound by  $19.5 \text{ kcal mol}^{-1}$ . The results of both sets of complexes are in qualitative agreement with similar results from studies on  $Cl^- \cdot HOCl$  complexes.<sup>15</sup> For  $Br^- \cdot HOBr$  type complexes, we find that the minimum energy structure involves complexation through the hydrogen of the acid. The  $Br^- \cdot HOBr$  complex is predicted to be bound by  $19.5 \text{ kcal mol}^{-1}$ .

**Acknowledgment.** We thank S. Aliosio, D. Good, Y. Li, and B. Putnam for helpful discussions.

#### References and Notes

- (1) Anderson, J. G. *Annu. Rev. Phys. Chem.* **1987**, *38*, 489.
- (2) Hamill, P.; Toon, O. B. *Phys. Today* **1991**, *44*, 34.
- (3) Rowland, F. S. *Annu. Rev. Phys. Chem.* **1991**, *42*, 731.
- (4) Randeniya, L. K.; Vohralik, P. F.; Plumb, K.; Ryan, K. R. *J. Geophys. Res. Atmos.* **1997**, *102*, 23543.
- (5) Hanson, D. R.; Ravishankara, A. R. *Geophys. Res. Lett.* **1995**, *22*, 385.
- (6) Hanson, D. R.; Ravishankara, J. *Phys. Chem.* **1992**, *96*, 2682.
- (7) Abbatt, J. P. D.; Molina, M. *Geophys. Res. Lett.* **1992**, *19*, 461.
- (8) Opplinger, R.; Allan, A.; Rossi, M. J. *J. Phys. Chem. A* **1997**, *101*, 1903.
- (9) Abbatt, J. P. D. *Geophys. Res. Lett.* **1994**, *21*, 665.
- (10) Allan, A.; Opplinger, R.; Rossi, M. J. *J. Geophys. Res.* **1997**, *102*, 23529.
- (11) Chu, L.; Chu, L. *J. Phys. Chem. A* **1999**, *103*, 691.
- (12) Abbatt, J. P.; Bayer, K. D.; Fucaloro, A. F.; McMahon, J. R.; Wooldridge, P. J.; Zhang, R.; Molina, M. J. *J. Geophys. Res.* **1992**, *97*, 15819.
- (13) Abbatt, J. P. D.; Molina, M. J. *Phys. Chem.* **1992**, *96*, 7074.
- (14) Haas, B. M.; Crellin, K. C.; Kuwata, K. T.; Okumura, M. *J. Phys. Chem.* **1994**, *98*, 6740.
- (15) Francisco, J. S. *Chem. Phys. Lett.* **1996**, *260*, 485.
- (16) Richardson, S. L.; Francisco, J. S.; Mebel, A. M.; Morokuma, K. *Chem. Phys. Lett.* **1997**, *270*, 395.
- (17) Eigen, M.; Kustin, K. *J. Am. Chem. Soc.* **1962**, *84*, 1355.
- (18) Choi, J.; Kuwata, K.; Cao, Y.; Okumura, M. *J. Phys. Chem. A* **1998**, *102*, 503.
- (19) Cambariza, J. E.; Kestner, N. R.; Jortner, J. *J. Phys. Chem.* **1994**, *100*, 2851.
- (20) Xantheas, S. *J. Phys. Chem.* **1996**, *100*, 9703.
- (21) Ayotte, P.; Weddle, G. H.; Kim, J.; Johnson, M. A. *J. Am. Chem. Soc.* **1998**, *120*, 12361.
- (22) Zhao, X. G.; Gonzalez-Lafont, A.; Truhlar, D. G.; Steckler, R. *J. Chem. Phys.* **1991**, *94*, 5544.
- (23) Schindler, T.; Berg, C.; Borg, C.; Niedner-Schatteburg, G.; Bondybex, V. E. *J. Phys. Chem.* **1990**, *99*, 12434.
- (24) Hirota, K.; Mizuse, S.; Yanabe, S. *J. Phys. Chem.* **1988**, *92*, 3943.
- (25) Larson, J. W.; McMahon, T. B. *J. Am. Chem. Soc.* **1984**, *106*, 517.
- (26) Shimanouchi, T. *Tables of Molecular Vibrational Frequencies Consolidated*; National Bureau of Standards: Gaithersburg, MD, 1972; Vol. 1, pp 1–160.
- (27) Ayotte, P.; Bailey, C. G.; Weddle, G. H.; Johnston, M. A. *J. Phys. Chem. A* **1998**, *102*, 3067.
- (28) Schwager, I.; Arkell, A. *J. Am. Chem. Soc.* **1967**, *89*, 6006.
- (29) Wang, T. X.; Margerum, D. W. *Inorg. Chem.* **1994**, *33*, 1050.
- (30) Cotton, F. A.; Wilkinson, G. *Advanced Inorganic Chemistry*, 5th ed.; Wiley: New York, 1988; p 577.
- (31) Ogawa, Y.; Takahashi, O.; Kikuchi, O. *J. Mol. Struct. (THEOCHEM)* **1998**, *429*, 187.